Technical report from Automatic Control at Linköpings universitet

Online Estimation of Ship's Mass and Center of Mass Using Inertial Measurements

Jonas Linder*, Martin Enqvist*, Thor I. Fossen†, Tor Arne Johansen†, Fredrik Gustafsson*

Division of Automatic Control

E-mail: jonas.linder@liu.se, maren@isy.liu.se, thor.fossen@ntnu.no, tor.arne.johansen@itk.ntnu.no, fredrik@isy.liu.se

13th March 2015

Report no.: LiTH-ISY-R-3081
Submitted to the 10th IFAC Conference on Manoeuvring and Control of Marine Craft

Address:
*Department of Electrical Engineering
Linköpings universitet
SE-581 83 Linköping, Sweden

†Centre for Autonomous Marine Operations and Systems (AMOS),
Department of Engineering Cybernetics
Norwegian University of Science and Technology
NO-7491 Trondheim, Norway

WWW: http://www.control.isy.liu.se

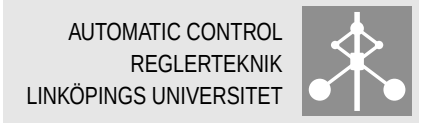

Abstract

A ship's roll dynamics is sensitive to the mass and mass distribution. Changes in these physical properties might introduce unpredictable behavior of the ship and a worst-case scenario is that the ship will capsize. In this paper, a recently proposed approach for online estimation of mass and center of mass is validated using experimental data. The experiments were performed using a scale model of a ship in a wave basin. The data was collected in free run experiments where the rudder angle was recorded and the ship's motion was measured using an inertial measurement unit. The motion measurements are used in conjunction with a model of the roll dynamics to estimate the desired properties. The estimator uses the rudder angle measurements together with an instrumental variable method to mitigate the influence of disturbances. The experimental study shows that the properties can be estimated with quite good accuracy but that variance and robustness properties can be improved further.

Keywords: modelling, identification, operational safety, inertial measurement unit, identifiability, centre of mass, physical models, accelerometers, gyroscopes, marine systems

1 Introduction

In marine vessels, mathematical models are nowadays commonly used to increase performance or accuracy. A good model is essential, for instance, in model-based control where a poor model will affect the performance negatively (Skogestad and Postlethwaite, 2005), or in decision supp-ort systems where an error in the model might result in bad advice. Ships have time-dependent properties and by estimating these online, a higher model accuracy can be achieved. One example is the mass of a container ship being changed due to loading of containers. The dynamic behavior of the ship is affected by these properties and a large variation of certain properties might be safety critical.

A ship's roll dynamics is very sensitive to changes in the loading conditions and a worst-case scenario is that the ship will capsize (Fossen, 2011; Tannuri et al., 2003). Iseki and Terada (2001) study the problem of estimating the directional wave spectrum from ship motion. The wave spectrum can then be used to simulate a ship's response over time, to apply control or to suggest appropriate actions. This is basically an inverse problem and the result is dependent on the ship's mass. Inaccurate knowledge of the ship's mass, and thus of the model, might lead to an inaccurate wave spectrum, which in the end might lead to poor performance if the wave spectrum is used in the earlier mentioned control or decision support systems.

Perez (2005) presents methods for ship roll stabilization or ship roll reduction systems using model-based control. The model used in the approach is a linear maneuvering model where the parameters are assumed to be known. The effects of model errors are not investigated, but due to changes in the ship roll dynamics shown in, for instance, Fossen (2011) and Tannuri et al. (2003), it seems likely that a significant change in mass will affect the ship dynamics and that online estimation of the mass would make it possible to increase the performance of the controller.

In most mechanical systems, the mass is actually one of the properties that influence the dynamics the most. If the forces acting on the system are not known, it is difficult to uniquely determine the mass with motion data only since large forces acting on a heavy system cannot be distinguished from small forces acting on a light system. This ambiguity can be overcome with special experiments where the forces acting on the system are known, or by introducing sensors that can measure the forces. However, introducing special sensors or experiments is in many cases intractable or too expensive.

Online mass estimation for vehicles has been considered in especially automotive applications, see for instance, Fathy et al. (2008). However, for a ship, there are additional challenges that are not present in ground vehicles due to the complex interaction with the water. For example, there are strong couplings between the ship's degrees of freedom and the motion of the ship is strongly affected by the environmental disturbances.

An approach to mitigate the influence of the environmental disturbances using an instrumental variable (IV) method and the rudder angle was proposed in Linder et al. (2014b) and Linder et al. (2014a). A simplified model of the roll dynamics was used and it was assumed that only motion data from an inertial measurement unit (IMU) together with the rudder angle were available. In Linder et al. (2015), an extended model was derived from well-established results in literature to also consider the strong couplings in ships.

This paper presents an experimental study of online estimation of a ship's mass and center of mass using the recently proposed approach derived in Linder et al. (2015) with data recorded from a scale ship operated in a basin. The data was collected under moderate sea conditions in free run experiments where the scale model was controlled manually using a joystick. The goals of the study are to validate the model and method using real data, and to evaluate the properties, such as the accuracy, of the estimator. Furthermore, to investigate the influences from disturbances, the IV estimator is compared with a least-squares estimator.

The outline of this paper is: In Section 2, the model used in the approach is introduced. In Section 3, the model is discretized, identifiability issues are discussed and an IV estimator is suggested to estimate the model. Sections 4 and 5 introduce the experimental setup and the data. Finally, the results are presented and discussed in Section 6 and conclusions are given in Section 7.

2 Problem Formulation

The roll dynamics is particularly sensitive to the loading condition and to get a connection from the rudder angle to the roll dynamics, the four degree-of-freedom (DOF) surge–sway–roll–yaw maneuvering model with rudder input developed and discussed in Blanke and Christensen (1993) and Perez (2005) is used as a foundation. The model can be written in the nonlinear state-space form

$$\tilde{\boldsymbol{M}}\dot{x} = F(x,\delta) + \boldsymbol{\tau} \tag{1}$$

where $\boldsymbol{\tau}$ is the environmental disturbance, $\tilde{\boldsymbol{M}}$ is the inertia matrix, $F(x,\delta)$ is a nonlinear state transition function and δ is the rudder angle. The states are given by

$$x^T = [\phi,\ \psi,\ v,\ p,\ r] \tag{2}$$

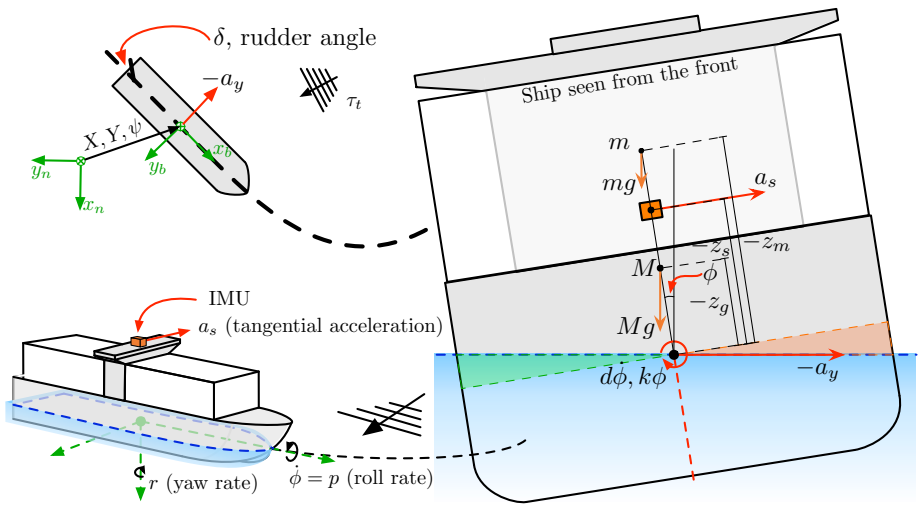

Figure 1: A sketch of a ship performing a turn which results in an unknown acceleration a_y acting on the CR.

where ϕ is the roll angle and ψ is the yaw angle expressed in a Earth-fixed coordinate system which is assumed to be inertial. Furthermore, v is the linear surge speed, p is the angular velocity about the roll axis and r is the angular velocity about the yaw axis expressed in a body-fixed coordinate system.

Since the actual forces acting on the ship are unknown and we instead work with measurement of the motion, we will estimate the change in mass and change in center of mass (CM). The total mass of the ships is split into a nominal mass M and a load mass m with CMs given by z_g and z_m, respectively, see Figure 1 for a sketch.

To get a model of the roll subsystem, the model (1) is linearized about $\bar{x} = 0$ and $\bar{\delta} = 0$ where it assumed that that the surge component can be decoupled due to much slower dynamics and that the ship is port–starboard and fore-aft symmetric, i.e. $\bar{y}_g = \bar{x}_g = 0$. The third row of this linearized system is after a few manipulations given by

$$\begin{aligned} A_1\ddot{\phi} = &- (k + Mgz_g + mgz_m)\phi - d\dot{\phi} \\ &+ (K_{\dot{v}} + Mz_g + mz_m)\dot{v} + (K_{ur} + Mz_g + mz_m)Ur \\ &+ K_\delta \delta + \tau \end{aligned} \tag{3}$$

where

$$A_1 = A_x + Mz_g^2 + mz_m^2 = I_x - K_{\dot{p}} + Mz_g^2 + mz_m^2, \tag{4}$$

I_x is the ship's inertia about the CM, $K_{\dot{p}}$ and $K_{\dot{v}}$ are added moment of inertia, K_{ur} is the Coriolis coefficient due to added moment of inertia and τ is the process disturbance. Here, the two lumped parameters

$$k = -K_{\phi uu}U^2 + \rho g \nabla \overline{GM}_T - Mgz_g - mgz_m, \tag{5a}$$

and

$$d = -K_p - K_{|u|p}|U| \tag{5b}$$

have been introduced to get an identifiable model structure. The parameter k should be thought of as representing the physical restoring properties of the ship, for instance, being dependent on factors such as the hull shape, while the term $Mgz_g + mgz_m$ represents the influence by the mass and its location on the restoring properties. For a thorough derivation of the model, see Linder et al. (2015) or Linder (2014).

2.1 Sensors – Intertial Measurement Unit (IMU)

The ship's motion is assumed to be observed with an IMU and the IMU's position can be seen in Figure 1. The IMU measurements are

$$y_{1,t} = p_t \quad + b_{1,t} + e_{1,t} = \dot{\phi}_t + b_{1,t} + e_{1,t} \tag{6a}$$
$$y_{2,t} = a_{s,t} + b_{2,t} + e_{2,t} \tag{6b}$$
$$y_{3,t} = -r_t + b_{3,t} + e_{3,t} \tag{6c}$$
$$\tag{6d}$$

where $p_t = \dot{\phi}_t$ is the sampled system's angular velocity about the roll axis, $a_{s,t}$ is the tangential acceleration after sampling, r_t is the sampled system's angular velocity about the yaw axis, $b_{i,t}, i = 1, 2, 3$, are sensor biases and $e_{i,t}, i = 1, 2, 3$, are measurement noise. Assuming that the roll angle ϕ is small, the acceleration sensed by the IMU is

$$a_s = z_s\ddot{\phi} + g\phi - a_y, \tag{7}$$

where $-z_s$ is the distance from the center of rotation (CR) to the origin of the IMU coordinate system. The first term is the contribution from the angular acceleration, the second term is due to gravity and the third term is the acceleration of the CR in the xy–plane in the earth-fixed frame. Note that the identity $p = \dot{\phi}$ is not valid in general and only holds due to the assumption of small roll angles.

2.2 A Limited Sensor Approach

With $\dot{v}$, r, δ and τ as inputs, the model (3) is a mass–spring–damper model. The issue is that $\dot{v}$ is unknown but an alternative model can be formed by eliminating $\dot{v}$. The key to this elimination is the known relation between the measured tangential acceleration a_s defined in (7), the acceleration a_y and the signal $\dot{v}$ (Linder et al., 2015). The acceleration a_y of the ship in the Earth-fixed xy–plane has two parts, firstly a contribution from the sway motion and secondly due to the angular velocity about the yaw axis. The total sway acceleration is given by

$$a_y = \dot{v} + Ur \tag{8}$$

which means that $\dot{v}$ is indirectly measured by the tangential acceleration a_s. Combining (8) with (7), solving for $\dot{v}$ and substituting it into (3) give

$$\begin{aligned} A_2\ddot{\phi} = &-(k - K_{\dot{v}}g)\phi - d\dot{\phi} \\ &-(K_{\dot{v}} + Mz_g + mz_m)a_s + (K_{ur} - K_{\dot{v}})Ur \\ &+ K_\delta\delta + \tau \end{aligned} \tag{9}$$

where

$$A_2 = A_x + Mz_g(z_g - z_s) + mz_m(z_m - z_s) - K_{\dot{v}}z_s \tag{10}$$

If the surge speed U is assumed to be constant, this model can be further simplified by introducing the lumped parameter $K_r = (K_{ur} - K_{\dot{v}})U$ which gives the model

$$\begin{aligned} A_2\ddot{\phi} = &-(k - K_{\dot{v}}g)\phi - d\dot{\phi} \\ &-(K_{\dot{v}} + Mz_g + mz_m)a_s + K_r r + K_\delta\delta + \tau \end{aligned} \tag{11}$$

To enable estimation of the CR, the CMs and position of the IMU are expressed as

$$z_g = \bar{z}_g + z_f, \quad z_m = \bar{z}_m + z_f \quad \text{and} \quad z_s = \bar{z}_s + z_f \tag{12}$$

where z_f is the distance from the CR to the body-fixed coordinate system and $\bar{z}_i, i = g, m, s$ are relative to the body-fixed coordinate system. The parameters k, d and K_r are all dependent on the surge speed U but the dependencies are not written out to ease notation. Finally, note that even though the use of the proposed model avoids building a model of the entire ship, it introduces some new challenges. Most notably, the signals r, a_s and ϕ are all correlated with the disturbance τ, i.e. all signals will be affected by the waves, due to the coupling in the real system. This complicates the parameter estimation since it is similar to closed-loop system identification (Linder, 2014).

3 Parameter Estimation

When it comes to estimation of the parameters in (11) there are a lot of details that have to be considered. In this section, the most important points are summarized. For a more detailed discussion, see Linder (2014).

3.1 Discretization Using Physical Parameters

The model (11) with the output $y = \dot{\phi}$ can be written on transfer function form and be discretized using the bilinear transform $\mathsf{p} = 2/T(\mathsf{q}-1)/(\mathsf{q}+1)$ where T is the sample period, p is the differentiation operator and q is the shift operator. This gives the discrete-time model

$$y_t = G_d(\mathsf{q})(a_{s,t} + F_{r,d} r_t + F_{\delta,d}\delta_t + \tau_t) \tag{13}$$

where

$$G_d(\mathsf{q}) = \frac{\bar{\beta}_0(1-\mathsf{q}^{-2})}{1+\bar{\alpha}_1\mathsf{q}^{-1}+\bar{\alpha}_2\mathsf{q}^{-2}}, \; F_{\delta,d} = \frac{\bar{\gamma}_0}{\bar{\beta}_0}, \; F_{r,d} = \frac{\bar{\kappa}_0}{\bar{\beta}_0}, \tag{14}$$

$$\begin{aligned} \bar{\alpha}_1 &= \frac{2(k-K_{\dot{v}}g)T^2 - 8A_2}{\mathcal{A}_2(\bar{\vartheta}_p)}, \; \bar{\alpha}_2 = \frac{-2dT + (k-K_{\dot{v}}g)T^2 + 4A_2}{\mathcal{A}_2(\bar{\vartheta}_p)} \\ \bar{\beta}_0 &= -\frac{2T(K_{\dot{v}} + Mz_g + mz_m)}{\mathcal{A}_2(\bar{\vartheta}_p)}, \; \bar{\kappa}_0 = \frac{2TK_r}{\mathcal{A}_2(\bar{\vartheta}_p)}, \; \bar{\gamma}_0 = \frac{2TK_\delta}{\mathcal{A}_2(\bar{\vartheta}_p)}, \end{aligned} \tag{15}$$

and $\mathcal{A}_2(\bar{\vartheta}_p) = 2dT + (k - K_{\dot{v}}g)T^2 + 4A_2$. By introducing

$$\mu_t^T = \left[a_{s,t} - a_{s,t-2}, \; r_t - r_{t-2}, \; \delta_t - \delta_{t-2}\right], \tag{16}$$

$$g_\vartheta(\bar{\vartheta}_p) = \left[\bar{\alpha}_1(\bar{\vartheta}_p), \; \bar{\alpha}_2(\bar{\vartheta}_p), \; \bar{\beta}_0(\bar{\vartheta}_p), \; \bar{\kappa}_0(\bar{\vartheta}_p), \; \bar{\gamma}_0(\bar{\vartheta}_p)\right]^T \tag{17}$$

and

$$\varphi_t^T = \left[-y_{t-1}, -y_{t-2}, \mu_{1,t}, \mu_{2,t}, \mu_{3,t}\right], \tag{18}$$

the discrete-time model (13) can be written as the linear regression

$$y_t = \varphi_t^T g_\vartheta(\bar{\vartheta}_p) + \tilde{\tau}_t \tag{19}$$

3.2 Identifiability Issues – Using Multiple Datasets

The subject of uniquely determining the parameters in a chosen model structure is both connected to the model structure considered and the informativity of the data set used for identification (Bazanella et al., 2010). Assuming that g and $\bar{z}_s$ are known, the model (11) with $\dot{\phi}$ as an output is not identifiable with respect to the parameters

$$\bar{\vartheta}_p^T = \left[M,\ \bar{z}_g,\ k,\ \bar{A}_x,\ d,\ K_r,\ K_{\dot{v}},\ K_\delta,\ z_f,\ m,\ \bar{z}_m\right], \tag{20}$$

using a single dataset due to over-parameterization. To overcome this identifiability issue, more information has to be introduced. In this work, the extra information is introduced through the datasets

$$Z_n = (y_t, u_t, \delta_t)_{t=1+t_n}^{N_n+t_n} \text{ and } Z_c = (y_t, u_t, \delta_t)_{t=1+t_c}^{N_c+t_c} \tag{21}$$

which are called the nominal and calibration dataset, respectively. The nominal dataset is collected with a known nominal mass M with the CM $\bar{z}_g$ while the calibration dataset has a different known mass and the total CM expressed using the load mass $m = m_c$ with the CM $\bar{z}_m = \bar{z}_c$. Then during normal operation, the loaded dataset

$$Z_l = (y_t, u_t, \delta_t)_{t=1+t_l}^{N_l+t_l} \tag{22}$$

is collected and all parameters can be estimated simultaneously using the joint model

$$\boldsymbol{y}_t = \boldsymbol{\varphi}_t^T \boldsymbol{\theta}(\tilde{\vartheta}_p) + \tilde{\boldsymbol{\tau}}_t \tag{23}$$

where $\boldsymbol{y}_t = [y_t^n, y_t^c, y_t^l]^T$,

$$\boldsymbol{\theta}(\tilde{\vartheta}_p) = \left[g_\vartheta^T(\bar{\vartheta}_p^n),\ g_\vartheta^T(\bar{\vartheta}_p^c),\ g_\vartheta^T(\bar{\vartheta}_p^l)\right]^T, \quad \boldsymbol{\varphi}_t = \begin{bmatrix} \varphi_t^n & 0 & 0 \\ 0 & \varphi_t^c & 0 \\ 0 & 0 & \varphi_t^l \end{bmatrix}, \tag{24}$$

$$\tilde{\vartheta}_p = [\overbrace{M,\ \bar{z}_g,\ m_c,\ \bar{z}_c}^{\tilde{\vartheta}_{p,1}\ \text{(known)}},\ \overbrace{k,\ A_x,\ d,\ K_r,\ K_{\dot{v}},\ K_\delta,\ z_f,\ m,\ \bar{z}_m}^{\tilde{\vartheta}_{p,2}\ \text{(unknown)}}]^T, \tag{25}$$

$$\bar{\vartheta}_p^n = \bar{\vartheta}_p|_{m=\bar{z}_m=0},\ \bar{\vartheta}_p^c = \bar{\vartheta}_p|_{m=m_c\bar{z}_m=\bar{z}_c},\ \bar{\vartheta}_p^l = \bar{\vartheta}_p \tag{26}$$

and the subscripts $i = n, c, l$ correspond to the nominal, calibration and loaded datasets, respectively. Note that the starting times $t_i, i = n, c, l$ are used to emphasize that these datasets are not collected at the same time. For more details, see Linder et al. (2015) or Linder (2014).

3.3 The Instrumental Variable Estimator

There are two terms contributing to the output of (23), one containing information about the interesting input-output relation and the second containing a contribution from disturbances. An instrumental variable (IV) method uses instruments to extract the interesting information from the data. In principle, the interesting information is estimated by requiring that the sample covariance between the instruments and the prediction error should be zero (Söderström and Stoica, 1989). A good instrument should in this case be correlated with the motion induced by the rudder but be uncorrelated with the process disturbance τ, the sensor biases $b_{i,t}$, and the measurement noises $e_{i,t}$. This idea is implemented using a version of the extended IV method, where the parameters are found by computing

$$\hat{\vartheta} = \underset{\vartheta}{\operatorname{argmin}} \left\| Y_N - \Phi_N \boldsymbol{\theta}(\vartheta) \right\|^2, \tag{27}$$

$$\Phi_N = [\boldsymbol{\zeta}_1 \dots \boldsymbol{\zeta}_N] \begin{bmatrix} \boldsymbol{\varphi}_1^T \\ \vdots \\ \boldsymbol{\varphi}_N^T \end{bmatrix}, \; Y_N = [\boldsymbol{\zeta}_1 \dots \boldsymbol{\zeta}_N] \begin{bmatrix} \boldsymbol{y}_{,1} \\ \vdots \\ \boldsymbol{y}_{,N} \end{bmatrix}, \; \boldsymbol{\zeta}_t = \begin{bmatrix} \frac{\zeta_t^n}{N_n} & 0 & 0 \\ 0 & \frac{\zeta_t^c}{N_c} & 0 \\ 0 & 0 & \frac{\zeta_t^l}{N_l} \end{bmatrix} \tag{28}$$

and $\|x\|^2 = x^T x$. The superscript $i = n, c, l$, corresponds to the datasets defined in Section 3.2 and for brevity, $i = n, c, l$ is not explicitly written at all places in this section. See, for instance, Söderström and Stoica (1989) or Ljung (1999) for more details on the instrumental variable method.

The method presented in this section is based on the method of Gilson et al. (2006) where the parameters are estimated in an iterative scheme. In each iteration, the instruments are created by simulating the inputs and the outputs from the rudder angle by using the latest parameter estimates and the iterations are terminated when the parameters have converged.

In the j^{th} iteration, firstly, $\hat{\vartheta}_p^{i,j}$ are estimated using the vectors of instruments from the $j-1^{\text{th}}$ iteration. To create the instruments, the output and inputs of (13) are simulated with δ_t^i as input, which gives the signals

$$\hat{y}_t^{i,j} = \hat{G}_{\delta y,d}^{i,j}(\mathsf{q})\delta_t^i, \; \hat{a}_{s,t}^{i,j} = \hat{G}_{\delta a_s,d}^{i,j}(\mathsf{q})\delta_t^i \text{ and } \hat{r}_t^{i,0} = \hat{G}_{\delta r,d}^{i,0}(\mathsf{q})\delta_t^i \tag{29}$$

and the instrument vectors are created according to

$$\begin{aligned} \zeta_t^{i,j} = \big[& \hat{y}_t^{i,j} \dots \hat{y}_{t-n_y+1}^{i,j}, \; \hat{\mu}_{1,t}^{i,j} \dots \hat{\mu}_{1,t-n_{a_s}+1}^{i,j}, \\ & \hat{\mu}_{2,t}^{i,j} \dots \hat{\mu}_{2,t-n_r+1}^{i,j}, \; \mu_{3,t}^{i} \dots \mu_{3,t-n_\delta+1}^{i} \big]^T \end{aligned} \tag{30}$$

where the constants n_k, $k = y, a_s, r, \delta$, are the number of time lags (including the non-delay signal) included in $\zeta_t^{i,j}$, for instance, $n_\delta = 0$ means that $\mu_{3,t}$ is not included in $\zeta_t^{i,j}$. In the initializing (0^{th}) iteration, the transfer functions of (29) are blackbox models estimated from data. In the refining steps, the transfer functions of (29) are given by

$$\hat{G}_{\delta y,d}^{i,j} = \frac{G_d^{i,j}}{1 - G_d^{i,j} F_{y,d}^{i,j}} \left[(F_{r,d}^{i,j} - U)\hat{G}_{\delta r,d}^{i,0} + F_{\delta,d}^{i,j} \right], \tag{31}$$

$$\hat{G}_{\delta a_s,d}^{i,j} = \frac{G_d^{i,j}}{1 - G_d^{i,j} F_{y,d}^{i,j}} \left[F_{\delta,d}^{i,j} + F_{r,d}^{i,j}\hat{G}_{\delta r,d}^{i,0} \right] + \frac{U\hat{G}_{\delta r,d}^{i,0}}{1 - F_{y,d}^{i,j} G_d^{i,j}}, \tag{32}$$

where $\hat{G}_{\delta r,d}^{i,0}$ are the blackbox models estimated from data in the initialization step and the dependencies on q and $\hat{\vartheta}_p^{i,j}$ have been dropped for brevity.

3.4 Summary of the Approach

In this work, the ship's current mass and CM are found by online estimation of the deviation from the nominal mass M and CM $\bar{z}_g$. This is necessary since the approach uses motion data from an IMU. The drawback for not knowing the forces acting on the ship is the requirement of *a priori* information. The necessary information is:

- A nominal dataset collected with a known mass M and CM $\bar{z}_g$
- A calibration dataset collected with known change in mass m_c and change in CM $\bar{z}_c$
- The position of the IMU $\bar{z}_s$

Finally, the loaded dataset is collected during normal operation and the change in mass m and change in CM $\bar{z}_m$ can be estimated simultaneously with the other parameters according to Section 3.3. Note that the required position $\bar{z}_i, i = g, c, s$ are in relation to the body-fixed coordinate system chosen by the user and that the CR is estimated.

4 Experimental Setup

The experiments were performed in the small wave basin ($40 \times 6.45 \times 1.5$ m – length × width × depth) of the *Marine Cybernetics Laboratory* (MCLab) at the Norwegian University of Science and Technology (NTNU) in Trondheim.

An overview of the experimental setup can be seen in Figure 2. The lines correspond to information flow where the arrows represent the flow direction. The

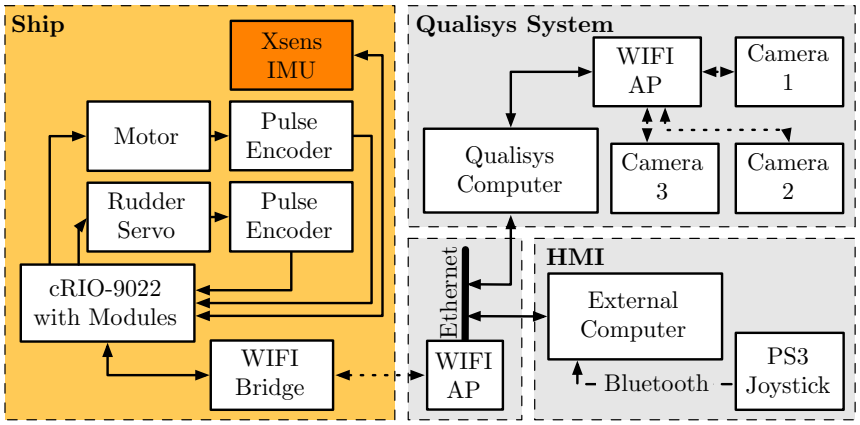

Figure 2: An overview of the information flow in the experimental setup. The arrows indicate the flow direction, a dotted line corresponds to WIFI communication and a solid line corresponds to any wired communication or signal. The system basically consisted of three computers communicating over ethernet and WIFI, the CompactRIO (cRIO) controller on the ship, the Qualisys computer and the external computer.

Table 1: "Our Lass II" in scale 1 : 24. Model parameters originating from Thys (2013).

Parameter	**Model**	**Unit**
Length between perpendiculars L_{pp}	0.8	m
Length at the waterline L_w	0.85	m
Beam B	0.3	m
Draft at COG D	0.144	m
Draft fore D_f	0.144	m
Draft aft D_a	0.144	m
Displacement Δ	22.04	kg
LCG from midship	0.125	m
$\overline{KG}$	0.146	m
$\overline{GM}_T$	0.018	m
Radius of Gyration in Roll K_{xx}/B	0.337	m
Radius of Gyration in Pitch K_{yy}/L	0.272	m
Radius of Gyration in Yaw K_{zz}/L	0.272	m

dashed line corresponds to bluetooth communication, dotted lines correspond to WIFI communication and solid lines correspond to any wired communication or signal. The system had three major components, the ship, the Qualisys real-time positioning system and the human-machine interface.

The scale model, hereafter called the ship, was a model of a fishing vessel called "Our Lass II" that is roughly 20 m long, see Figure 3. The ship was in scale 1 : 24 and the known physical quantities are listed in Table 1. The ship had a cRIO Controller that ran the LabVIEW Real-Time operating system and communicated via a WIFI bridge to the external computer that ran LabVIEW. The ship had its own propulsion and steering that were controlled through the onboard cRIO controller. The cRIO controller collected data from the three onboard sensors, an IMU, measuring angular velocities and linear accelerations, and two pulse encoders that were measuring the RPM of the motor and the steering angle, respectively. The IMU was an Xsens MTi-G that was equipped with a three-axes gyro and a three-axes accelerometer and it was mounted underneath the black box seen on top of the ship in Figure 3.

As can be seen in Figure 3, the ship is close to square in shape, which meant that for small changes in the roll angle, the wetted surface area should not change much. This implies that the restoring torque will be close to linear for a given forward speed (Journée and Massie, 2001). The position of the load was chosen to be on top of the black box covering the IMU. Since the distance from the CR ($>$ 20 cm) was large, the weights had quite a big impact on the roll dynamics and stability of the ship. In the lower right picture of Figure 3, a load mass of 2 kg was added to the ship and with this mass, it was barely stable, which resulted in a large constant roll angle. Due to this, the load masses were chosen to be 0.200 and 0.400 kg. These correspond to an increase of 0.91% and 1.81% in the total mass, respectively.

The external computer was used as a human-machine interface, plotting the ship's current status, logging data and taking commands from a joystick to control the ship.

Figure 3: Top: A side view of the scale model that was used in the experiments. The IMU was located underneath the black and gray box on the top. Left: The ship seen from the front. Note that the change in wetted surface due to a roll motion should be small since the ship is square in shape. Right: The ship was very sensitive to the loading condition. The picture shows the massive roll angle resulting from a load mass of 2 kg corresponding to a 9% increase in mass.

Table 2: A summary of the different cases.

	Nominal	**Calibration**	**Loaded**
Case 1	Nominal – 1	0.200 kg – 2	0.200 kg – 3
Case 2	Nominal – 1	0.200 kg – 3	0.400 kg – 4
Case 3	Nominal – 1	0.200 kg – 2	0.400 kg – 4

5 Datasets, Instruments, Noise Models and Initial Values

The data was collected in free run experiments where the ship was untethered and running by its own power. The propeller speed was kept constant and the ship was manually controlled with the joystick. The runs did not follow any particular trajectory and both short and long turns were performed while as much as possible of the basin was utilized. Several datasets were recorded for 0, 0.200 and 0.400 kg loads. In this paper, four datasets were used, one nominal set, two sets with 0.200 kg load mass and one with 0.400 kg load mass. The datasets were combined into three different cases according to Table 2. The datasets were sampled at 100 Hz, filtered through an FIR equiripple low-pass filter of order 20 with a cut-off frequency of 0.5 Hz and down-sampled to 50Hz resulting in a data length roughly between 1 800–3 300 samples per dataset. As an example, the filtered nominal dataset can be seen in Figure 4.

The acceleration of gravity g and the position $\bar{z}_s$ of the IMU in relation to the body-fixed coordinate system were both assumed to be known. Furthermore, the initial conditions were in all cases assumed to be

$$\begin{aligned} \tilde{\vartheta}_{p,2} &= [k,\ A_x,\ d,\ K_r,\ K_{\dot{v}},\ K_\delta,\ z_f,\ m,\ \bar{z}_m]^T \\ &= [9,\ 0.5,\ 0.1,\ -0.4,\ 1,\ -0.4,\ -0.018,\ 0,\ 0]^T \end{aligned} \tag{33}$$

In all iterations, the instruments (30) were created using the constants $n_y = 16$, $n_{a_s} = 16$, $n_r = 16$ and $n_\delta = 2$ for each dataset. The experiments were performed without using the wave maker but reflections of the bow waves on the walls of the basin were observed. This corresponds to sea states 1 and 2 (rippled and smooth waves) (Fossen, 2011).

6 Results

The instrumental variable method described in Section 3.3 was applied to each case in Table 2 and the results can be seen in Table 3. Note that the estimated parameters were roughly the same in all three cases. As expected, Case 1 had the best results of all the cases in Table 2, probably since the calibration dataset was similar to the loaded dataset, i.e. having the same mass and position. The estimated mass was less than 1 g away from the true value and the CM location had an error of less than 4 mm. Cases 2 and 3 were more realistic cases in a sense that the masses and the centers of gravity were different between the calibration and loaded datasets. The largest relative error in the mass estimation was 16.6 % which corresponds to 66.5 g or 0.3 % of the total mass of the ship.

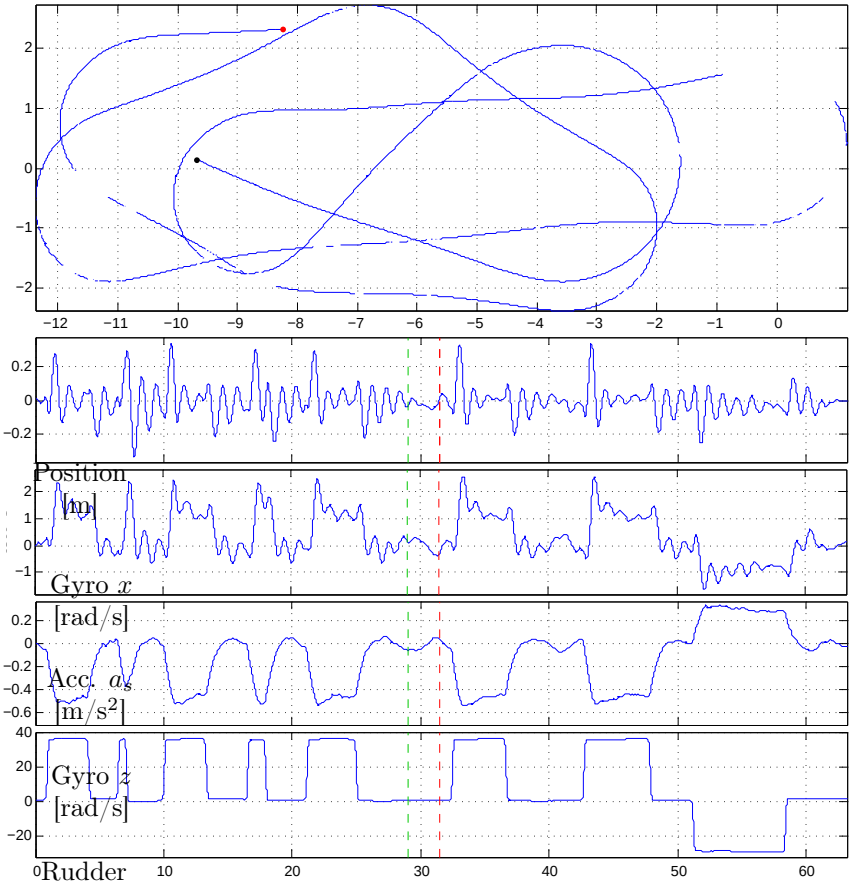

Figure 4: The nominal data after filtering. The dashed red and green lines correspond to the end of Case 1(a) and the start of Case 1(b), respectively.

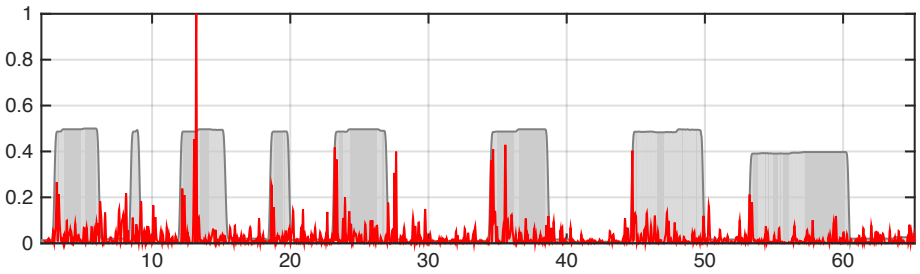

Figure 5: Red: The normalized residuals for the nominal dataset. Gray: The scaled absolute value of the rudder angle. The area between the rudder angle and the x–axis is filled to make the plot easier to read. Note that there are spikes at almost all the turn entries, which indicates that the model was not capturing all the dynamics. The magnitudes of these spikes are around 10 times larger than the average residual.

Table 3: Estimation results for IV estimator on the cases in Table 2. P: parameters, T: true values, I: initial values and E: the relative error. Here, the rows starting with 1,2,3,a and b correspond to the cases discussed in Section 6.

P	A_x	d	k	$-K_\delta$	$-K_r$	$K_{\dot{v}}$	$-z_f$	m	$-\bar{z}_m$
T	–	–	–	–	–	–	–	0.2000	0.2560
I	0.5000	0.1000	9.0000	0.4000	0.4000	1.0000	0.0180	0.0000	0.0000
1	0.1583	0.2685	9.0057	0.4822	2.0100	0.9607	0.0294	0.1997	0.2529
E	–	–	–	–	–	–	–	0.1338	1.212%
2	0.1566	0.2668	9.0067	0.4433	1.9911	0.9408	0.0293	0.3690	0.2426
E	–	–	–	–	–	–	–	7.7532	9.4842%
3	0.1571	0.2675	9.0021	0.4383	1.9995	0.9516	0.0294	0.3335	0.2671
E	–	–	–	–	–	–	–	16.631	0.3286%
a	0.1552	0.2411	8.9986	0.4821	2.0227	0.9376	0.0294	0.1629	0.2977
E	–	–	–	–	–	–	–	18.557	16.271%
b	0.2234	0.4395	8.9967	0.5042	2.3138	1.0350	0.0246	0.3005	0.1951
E	–	–	–	–	–	–	–	50.259	23.776%

To test the variation of the IV estimator the datasets of Case 1 were split into two cases. Case 1(a) roughly corresponded to the first half of the datasets and Case 1(b) roughly corresponded to the last half of the datasets. As an example, the end of the nominal datasets of Case 1(a) is indicated as the dashed red line in Figure 4. In the same way, the start of the nominal dataset of Case 1(b) is indicated as the dashed green line in Figure 4. In Case 1(a), the data lengths were 1576, 901 and 1276 samples after decimation for the nominal, calibration and loaded datasets, respectively. For Case 1(b), the corresponding numbers were 1701, 1026 and 1401. The estimation results can be seen with the indices A and B in Table 3. The maximum relative error, 54 % was quite large, however, it corresponds to less than 1 % of the total mass of the ship. Also, note that there might be a finite data effect since the datasets are quite short. Cases 2 and 3 had the same nominal and loaded datasets but different calibration datasets which was another indication that the variation was acceptable for the IV estimator. In Figure 5 the normalized residuals are plotted together with the scaled absolute value of the rudder angle. The figure shows clear deterministic components in the residuals with large spikes at the turn entries which indicates that there was unmodeled dynamics.

Note that no pre-processing, except for the lowpass-filtering, has been performed on the data. A side affect of using the IV method is that the biases in the measurements, in addition to the process disturbance and measurement noises, are automatically taken care of. The disturbances acting on the data, i.e. the sensor biases $b_{i,t}, i = 1, 2, 3$, the process disturbance τ and measurement noises $e_{i,t}, i = 1, 2, 3$, are quite important to consider and will introduce a bias in the estimator if they are neglected. To get an indication of the importance of the disturbances, the constrained least squares estimator, i.e. setting $\zeta_t^i = \varphi_t^i, i = n, c, l$, was used to compute the estimate and the result can be seen in Table 4. There is quite a significant difference compared to the IV estimator which performed better in all cases. Note that a constant heel angle, i.e. a that the mean of the roll angle is non-zero, only will be visible through the gravity-term in (7) and that this "bias" will be treated in the same way as a

Table 4: Estimation results for LS estimator on the cases in Table 2. P: parameters, T: true values, I: initial values and E: the relative error. Here, the rows starting with 1,2 and 3 correspond to the cases discussed in Section 6.

P	A_x	d	k	$-K_\delta$	$-K_r$	$K_{\dot{v}}$	$-z_f$	m	$-\bar{z}_m$
T	–	–	–	–	–	–	–	0.2000	0.2560
I	0.5000	0.1000	9.0000	0.4000	0.4000	1.0000	0.0180	0.0000	0.0000
1	0.1810	0.2739	9.0125	0.5828	2.1185	0.7861	0.0248	0.0574	0.6474
E	–	–	–	–	–	–	–	71.282	152.88%
2	0.1882	0.2830	9.0108	0.5827	2.1800	0.8256	0.0247	0.8602	0.1221
E	–	–	–	–	–	–	–	115.05	54.455%
3	0.1817	0.2802	9.0099	0.5886	2.1624	0.8185	0.0251	0.5580	0.1826
E	–	–	–	–	–	–	–	39.501	31.866%

sensor bias.

Figure 6 shows an estimate of the surge speed for the nominal dataset. The estimate was obtained using an extended Kalman smoother with a continuous turn model and position data from the available Qualisys positioning system. There is a clear variation of the surge velocity that is correlated to the rudder angle which meant that the assumption of constant velocity was violated. This might be one reason for the spikes in the residuals seen in Figure 5. However, the method managed to estimate the parameters fairly well and was thus robust against these variations.

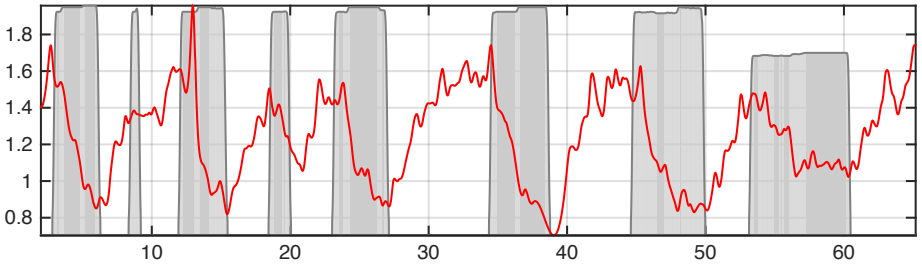

Figure 6: Variation in surge speed in the nominal dataset. Red: The surge velocity in m/s estimated from Qualisys data. Gray: The scaled absolute value of the rudder angle. The area between the rudder angle and the x–axis is filled to make the plot easier to read.

7 Conclusions and future work

In this paper, online estimation of a ship's mass and center of mass have been investigated using data collected from a scale ship and a model of the ships roll dynamics together with measurements from an inertial measurement unit. To mitigate impact of the disturbances, sensor biases and measurement noises, an iterative instrumental variable estimator was applied to the data with good results.

The residuals indicate a possibility for improved modeling. Future work includes analysis of the residuals to improve the performance of the estimator. Furthermore, it would be interesting to apply the method to data from full-scale test. In full-scale, the measured signals will be of the same magnitude as the scale model since acceleration does not scale, i.e an IMU in the same position on the ship will sense the same acceleration as the scale model and angular velocities will scale like $n^{-0.5}$ where n is the length scale factor. There are two big issues that need to be addressed in a full-scale test. Firstly, the parameters will be of different magnitude which might introduce numerical issues in the estimator. Secondly, the excitation level in the scale test were large to ensure informativity in the data and the question is if smaller excitations will significantly degrade the performance of the estimator. Since real-time estimates may not be needed all the time in an operational setting, one may incorporate logic to disable the estimator if low levels of excitation are degrading the quality of the estimates.

Acknowledgments

This work has been supported by the Vinnova Industry Excellence Center LINK-SIC and by the Research Council of Norway through the Centers of Excellence funding scheme, number 223254 - Centre for Autonomous Marine Operations and Systems (AMOS). The authors would like to thank Torgeir Wahl for his invaluable support during the wave basin tests.

References

Alexandre Sanfelice Bazanella, Michel Gevers, and Ljubiša Miškovic. Closed-loop identification of MIMO systems: A new look at identifiability and experiment design. *European Journal of Control*, 16(3):228–239, 2010. ISSN 0947-3580.

Mogens Blanke and Anders C Christensen. Rudder-roll damping autopilot robustness to sway-yaw-roll couplings. In *Proceedings of the 10th Ship Control Systems Symposium*, Ottawa, Canada, 1993.

H.K. Fathy, Dongsoo Kang, and J.L. Stein. Online vehicle mass estimation using recursive least squares and supervisory data extraction. In *American Control Conference, 2008*, pages 1842–1848, June 2008.

T. I. Fossen. *Handbook of Marine Craft Hydrodynamics and Motion Control*. Wiley, 2011. ISBN 9781119991496.

Marion Gilson, Hugues Garnier, Peter JW Young, Paul Van den Hof, et al. A refined IV method for closed-loop system identification. In *Proceedings of the 14th IFAC Symposium on System Identification*, pages 903–908, Newcastle, Australia, 2006.

T. Iseki and D. Terada. Bayesian estimation of directional wave spectra for ship guidance system. In *Proceedings of the International Offshore and Polar Engineering Conference*, volume 4, pages 577–582, 2001.

J. M. J. Journée and W. W. Massie. Offshore Hydromechanics, 2001. Lecture notes on offshore hydromechanics for Offshore Technology students, code OT4620.

Jonas Linder. *Graybox Modelling of Ships Using Indirect Input Measurements*. Linköping Studies in Science and Technology. Thesis 1681. 2014.

Jonas Linder, Martin Enqvist, and Fredrik Gustafsson. A closed-loop instrumental variable approach to mass and center of mass estimation using IMU data. In *Proceedings of the 53rd IEEE Conference on Decision & Control*, Los Angeles, CA, USA, December 2014a.

Jonas Linder, Martin Enqvist, Fredrik Gustafsson, and Johan Sjöberg. Identifiability of physical parameters in systems with limited sensors. In *Proceedings of the 19th IFAC World Congress*, Cape Town, South Africa, August 2014b.

Jonas Linder, Martin Enqvist, Thor I. Fossen, and Tor Arne Johansen. Modeling for IMU-based Online Estimation of Ship's Mass and Center of Mass. Technical Report 3082, Linköping University, The Institute of Technology, 2015.

L. Ljung. *System Identification: Theory for the User (2nd Edition)*. Prentice Hall, 1999. ISBN 0136566952.

T. Perez. *Ship Motion Control: Course Keeping and Roll Stabilisation Using Rudder and Fins*. Advances in Industrial Control Series. Springer-Verlag London Limited, 2005. ISBN 9781846281570.

S. Skogestad and I. Postlethwaite. *Multivariable Feedback Control: Analysis and Design*. Wiley, 2005. ISBN 9780470011676.

T.S. Söderström and P.G. Stoica. *System Identification*. Prentice Hall International Series In Systems And Control Engineering. Prentice Hall, 1989. ISBN 9780138812362.

E.A. Tannuri, J.V. Sparano, A.N. Simos, and J.J. Da Cruz. Estimating directional wave spectrum based on stationary ship motion measurements. *Applied Ocean Research*, 25(5):243–261, 2003.

Maxime Thys. *Theoretical and experimental investigation of a free running fishing vessel at small frequency of encounter*. PhD thesis, Norwegian University of Science and Technology, Trondheim, Norway, 2013.

Avdelning, Institution
Division, Department

Division of Automatic Control
Department of Electrical Engineering

Datum
Date

2015-03-13

Språk
Language

☐ Svenska/Swedish
☒ Engelska/English

☐ _____

Rapporttyp
Report category

☐ Licentiatavhandling
☐ Examensarbete
☐ C-uppsats
☐ D-uppsats
☒ Övrig rapport
☐ _____

ISBN
—

ISRN
—

Serietitel och serienummer
Title of series, numbering

ISSN
1400-3902

LiTH-ISY-R-3081

URL för elektronisk version

http://www.control.isy.liu.se

Titel
Title

Online Estimation of Ship's Mass and Center of Mass Using Inertial Measurements

Författare
Author

Jonas Linder, Martin Enqvist, Thor I. Fossen, Tor Arne Johansen, Fredrik Gustafsson

Sammanfattning
Abstract

A ship's roll dynamics is sensitive to the mass and mass distribution. Changes in these physical properties might introduce unpredictable behavior of the ship and a worst-case scenario is that the ship will capsize. In this paper, a recently proposed approach for online estimation of mass and center of mass is validated using experimental data. The experiments were performed using a scale model of a ship in a wave basin. The data was collected in free run experiments where the rudder angle was recorded and the ship's motion was measured using an inertial measurement unit. The motion measurements are used in conjunction with a model of the roll dynamics to estimate the desired properties. The estimator uses the rudder angle measurements together with an instrumental variable method to mitigate the influence of disturbances. The experimental study shows that the properties can be estimated with quite good accuracy but that variance and robustness properties can be improved further.

Nyckelord
Keywords

modelling, identification, operational safety, inertial measurement unit, identifiability, centre of mass, physical models, accelerometers, gyroscopes, marine systems